

See discussions, stats, and author profiles for this publication at: <https://www.researchgate.net/publication/231700329>

Synthesis, Characterization, and Surface Morphology of Pendant Polyhedral Oligomeric Silsesquioxane Perfluorocyclobutyl Aryl Ether Copolymers

ARTICLE *in* MACROMOLECULES · DECEMBER 2007

Impact Factor: 5.8 · DOI: 10.1021/ma071732f

CITATIONS

41

READS

35

4 AUTHORS, INCLUDING:



[Scott Iacono](#)

United States Air Force Academy

72 PUBLICATIONS 673 CITATIONS

SEE PROFILE



[Joseph Mark Mabry](#)

Air Force Research Laboratory

141 PUBLICATIONS 3,022 CITATIONS

SEE PROFILE



[Dennis W Smith](#)

University of Texas at Dallas

206 PUBLICATIONS 2,766 CITATIONS

SEE PROFILE

Synthesis, Characterization, and Surface Morphology of Pendant Polyhedral Oligomeric Silsesquioxane Perfluorocyclobutyl Aryl Ether Copolymers

Scott T. Iacono,[†] Stephen M. Budy,[†] Joseph M. Mabry,[‡] and Dennis W. Smith, Jr.,^{*,†}

Department of Chemistry and Center for Optical Materials Science and Engineering Technologies (COMSET), Advanced Materials Research Laboratory, Clemson University, Clemson, South Carolina 29634, and Air Force Research Laboratory, Propulsion Directorate, 10 East Saturn Boulevard, Edwards Air Force Base, California 93524

Received August 1, 2007; Revised Manuscript Received September 18, 2007

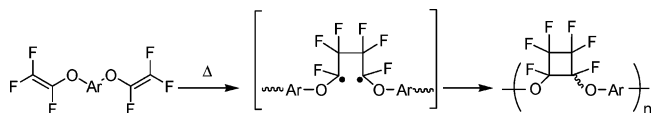
ABSTRACT: The synthesis and characterization of solution processable, semi-fluorinated perfluorocyclobutyl (PFCB) aryl ether polymers possessing covalently bound pendant polyhedral oligomeric silsesquioxanes (POSS) cages is reported. The synthesis of POSS aryl trifluorovinyl ether (TFVE) monomers was accomplished by the condensation of commercial monosilanolalkyl-POSS with a TFVE-functionalized chlorosilane. POSS TFVE monomers were elucidated by ¹H, ¹⁹F, ¹³C, and ²⁹Si NMR spectroscopy, ATR-FTIR analysis, and elemental (C, H, and F) combustion analysis. Bulk thermal copolymerization of POSS TFVE monomers afforded random and block PFCB aryl ether copolymers functionalized with various POSS loadings. Quantitative monomer conversion was monitored by ¹⁹F NMR, which produced copolymer number-average molecular weights (*M_n*) of (19.5–24.9) × 10³ (in CHCl₃ using polystyrene as standard) determined by gel permeation chromatography (GPC). Thermal properties of POSS PFCB aryl ether copolymers were evaluated by differential scanning calorimetry (DSC) and thermal gravimetric analysis (TGA). Transmission electron microscope (TEM) analysis of spin cast optically transparent, flexible POSS PFCB aryl ether copolymer films revealed the presence of 5–20 nm-sized POSS agglomerates. Optical profilometer analysis of spin and drop cast film surfaces exhibited a modest increase in surface roughness of POSS PFCB aryl ether copolymers as compared to PFCB aryl ether homopolymers without POSS inclusion. The POSS copolymers exhibited a modest increase in hydrophobicity as measured by static water contact angle analysis. Synthesis, characterization, thermal analysis, and unique surface features of POSS PFCB aryl ether copolymers are discussed.

Introduction

Fluoropolymers continue to be of global significance for a broad range of advanced material applications.¹ They are chemically inert, thermally robust, and possess low surface energies. Because they are intrinsically highly crystalline, they present costly processing challenges. On the other hand, perfluorocyclobutyl (PFCB) aryl ether polymers are an emerging class of next-generation processable, amorphous semi-fluorinated polymers.^{2,3} They are prepared by the condensate-free and radical-mediated [2+2] thermal cyclodimerization of aryl trifluorovinyl ether (TFVE) monomers to produce stereorandom PFCB aryl ether polymers (Scheme 1).⁴ PFCB aryl ether polymer systems possess tunable refractive indices, controllable glass transition temperatures, and are thermally robust. As a consequence, they are of particular interest in a multitude of material applications including high performance optics,³ photonics,⁵ electro-optics,⁶ atomic oxygen resistant coatings,⁷ and proton exchange membranes (PEMs) for fuel cells.⁸

Polyhedral oligomeric silsesquioxanes (POSS) are thermally robust, discreetly nanometer-sized building blocks for the development of high performance materials in aerospace⁹ as well as commercial markets.¹⁰ Numerous examples show that POSS can be either blended or covalently linked into a polymer.¹¹ These materials produce hybrid “ceramic-like” composites improving bulk properties including glass transition

Scheme 1. [2+2] Thermal Polymerization of TFVE Monomers Producing PFCB Aryl Ether Polymers



temperature, mechanical strength, thermal and chemical resistance, and ease of processing.

Thermal polymerization of the TFVE-functionalized octa-(aminophenyl)silsesquioxane (OAPS) with PFCB aryl ether oligomers has been reported to produce cross-linked materials possessing excellent thermal stability while retaining the optical integrity of the semi-fluorinated polymer.¹² PFCB aryl ether polymer thermoplastics and thermosets possessing siloxane linkages have also been prepared for high-temperature fluoro-silicone applications.¹³ Cross-linkable silane-modified PFCB aryl ether polymers have been used as thermosets in the lithographic patterning of electrodes for a gate dielectric in organic thin film transistors (OTFTs).¹⁴ We recently reported the preparation of POSS chain terminated PFCB aryl ether polymers with increased thermal stability and excellent solution processability and which afforded optically transparent, free-standing films.¹⁵ In this work, we show the preparation of PFCB aryl ether copolymers covalently bound to pendant POSS cages. The POSS PFCB aryl ether copolymers possess excellent processability and were easily solution spin and drop cast forming optically transparent, flexible films. The presence of POSS in the copolymer films unexpectedly produced an increase in surface roughness over the PFCB aryl ether homopolymers. As a consequence, these

* To whom correspondence should be addressed. E-mail: dwsmith@clemson.edu.

[†] Clemson University.

[‡] Air Force Research Laboratory.

copolymers showed enhanced water repellency due to POSS surface roughening in addition to increasing the hydrophobic hydrocarbon character of the POSS cages. Solution processable POSS PFCB aryl ether copolymers possessing this unique surface morphology were not known previously.

Experimental Section

General Procedures and Materials. Chemicals and solvents were purchased through Aldrich or Gelest and used without purification unless otherwise stated. HPLC grade THF was dried and deoxygenated using a Pure-Solv solvent purification system from Innovative Technologies. Flasks and syringes were flamed-dried under vacuum and allowed to cool in a desiccator prior to use. All reactions and solvent transfers were carried out under an atmosphere of nitrogen. 4-Bromo(trifluorovinyl)benzene (**1a**), 4,4'-bis(4-trifluorovinyl)biphenyl (**5**), and PFCB aryl ether homopolymer (**poly5**) were donated and are also commercially available from Tetramer Technologies, L.L.C. and distributed through Oakwood Chemicals, Inc. Analytical data for **poly5** are reported elsewhere.^{2b} Monosilanolcyclopentyl-POSS (**2a**), monosilanolisobutyl-POSS (**2b**), and octaisobutyl-POSS (used for blending with **poly5** and entitled **blend**) were donated by the Air Force Research Laboratory (Edwards AFB, CA) and are also commercially available through Hybrid Plastics. TFVE-functionalized chlorosilane (**3**) was prepared according to a previously published procedure.¹⁶

Instrumentation. ¹H, ¹³C{¹H}, ¹⁹F, and ²⁹Si NMR data were obtained on a JEOL Eclipse+ 300, and chemical shifts were reported in part per million (δ ppm). ¹H NMR was internally referenced to tetramethylsilane (δ 0.0), ¹³C{¹H} NMR chemical shifts were reported relative to the center peak of the multiplet for CDCl₃ (δ 77.0 (t)), and ¹⁹F NMR was referenced to CFCl₃. ²⁹Si NMR was referenced to tetramethylsilane (δ 0.0) and was recorded with inverse-gated proton decoupling with a 6 s pulse delay.

Attenuated total reflectance Fourier transform infrared (ATR-FTIR) analysis of neat samples was performed on a Thermo Nicolet Magna IR 550 FTIR spectrophotometer. Combustion analysis was obtained from Atlantic Microlab, Inc.

Gel permeation chromatography (GPC) data were collected in CHCl₃ using polystyrene as a standard (Polymer Labs Easical PS-2) using a Waters 2690 Alliance System with UV-vis detection at 35 °C. GPC samples were eluted in series through Polymer Labs PLGel 5 mm Mixed-D and Mixed-E columns.

Differential scanning calorimetry (DSC) analysis and thermal gravimetric analysis (TGA) were performed on a TA Q1000 instrument and Mettler-Toledo 851 instrument, respectively. Melting points were determined using a Mel-Temp melting point apparatus.

Contact angle measurements were performed using a Ramé-Hart 100-00 115 goniometer; deionized water drops (8–10 μ L) were manually dispensed from a 50 μ L syringe. Contact angle measurements were reported as an average of three areas on different portions of the film surface.

Transmission electron microscopy (TEM) micrographs and energy-dispersive X-ray spectroscopy (EDS) data were obtained from a Hitachi STEM HD-2000 200 kV at the CU Electron Microscope Facility. Surface analysis and roughness measurements (rms) were performed on a Zygo NewView 6300 3D white light optical profiling system.

Film Preparation. Two methods were used to prepare polymer films. For spin cast films, the dried polymer is initially applied in a minimal amount of THF onto a glass substrate and then spin coated at 2500–3000 rpm using a Chemat KW-4A spin coater. The polymer-coated substrate is dried in a vacuum oven at 60 °C for 24 h. For drop cast films, the polymer dissolved in a minimal amount of THF was dispensed onto a glass plate via a glass pipet, and a doctor blade was used to uniformly coat the surface. The polymer solution was allowed to evaporate in a glass enclosure for 48 h and then finally dried in an oven at 60 °C for an additional 24 h. Spin and drop cast film thicknesses were approximately 1–2

Table 1. Selected Properties of Polymers

poly	wt % (mol %) POSS ^a	$M_n \times 10^{-3}$ GPC ^b	M_w/M_n	T_g (°C) ^c	T_d (°C) ^d
4a-co-5	20 (7.1)	21.5	5.2	134	447 (439)
4b-co-5	10 (3.3)	24.9	1.4	133	452 (442)
4b-co-5	20 (6.6)	20.5	3.2	127	440 (438)
poly4a	100	6.6	3.5	131	
poly4b	100	6.3	2.5	138	
4b-b-5	10 (3.4)	21.9	3.4	149	450 (445)
4b-b-5	20 (6.7)	19.5	4.5	142	462 (444)
poly5	0	25.0	2.1	141	450 (446)

^a Percent of POSS monomer **4a** or **4b**. ^b GPC in CHCl₃ using polystyrene as standard. ^c DSC (10 °C min⁻¹) in nitrogen determined by third heating cycle. ^d TGA onset (10 °C min⁻¹) of chain extended polymers in nitrogen and air.

μ m thick and were measured by the Zygo NewView 6300 3D white light optical profiling system.

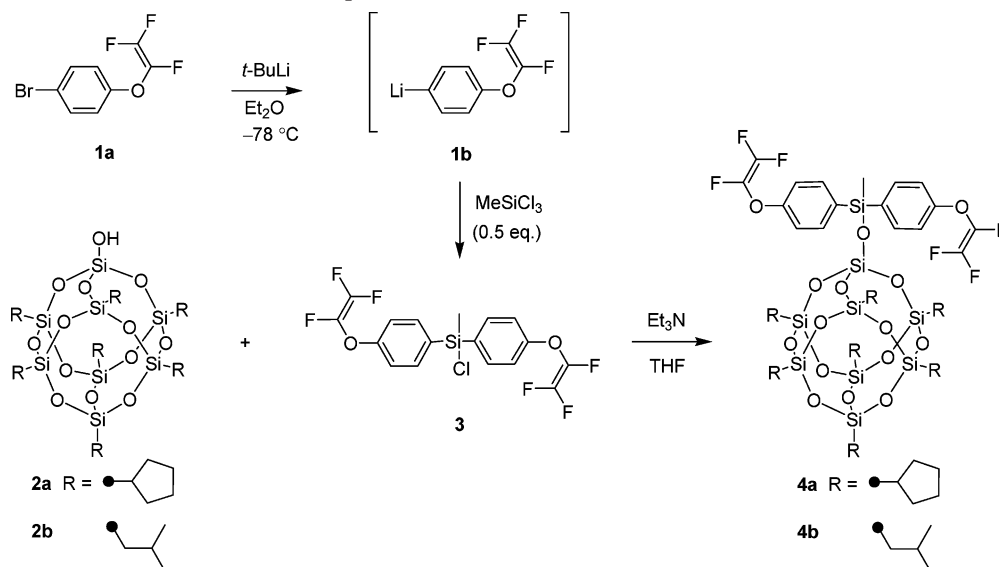
Synthesis of Monomer 4a. 4,4'-Bis(4-trifluorovinyl)biphenyl(methyl)chlorosilane (**3**) (510 mg, 1.20 mmol) in THF (2 mL) was added dropwise to monosilanolcyclopentyl-POSS (**2a**) (1.0 g, 1.09 mmol) and triethylamine (Et₃N) (184 μ L, 1.32 mmol) in THF (10 mL) at room temperature. After 24 h, the solution was filtered and concentrated under vacuum. The solid was then dispersed in methanol (100 mL), filtered, and dried under vacuum. Purification of the residue by flash chromatography on silica gel using 1% ethyl acetate–99% hexanes (v/v) for elution afforded the title compound as a white solid (410 mg, 29%). Mp 230 °C; ATR-FTIR (neat) ν 2949 (m), 1591 (w), 1497 (w), 1280 (m), 1079 (vs), 791 (w) cm⁻¹; ¹H NMR (CDCl₃, 300 MHz) δ 7.64 (d, J = 8.9 Hz, 4H), 7.12 (d, J = 8.9 Hz, 4H), 1.79–1.41 (m, 56H), 1.14–0.82 (m, 7H), 0.68 (s, 3H); ¹³C NMR (CDCl₃, 75 MHz) δ 156.5, 135.9, 133.5, 115.5, 27.4, 27.0, 22.3, –0.79; ¹⁹F NMR (CDCl₃, 283 MHz) δ –119.5 (dd, J = 95.5, 55.4 Hz, *cis*-CF=CF₂, 2F), –126.4 (dd, J = 111.9, 95.5 Hz, *trans*-CF=CF₂, 2F), –133.8 (dd, J = 111.9, 52.4 Hz, CF=CF₂, 2F); ²⁹Si NMR (CDCl₃, 59 MHz) δ –9.8, –65.3, –65.9, –107.9 (1:3:4:1). Anal. Calcd for C₅₂H₇₄F₆O₁₅Si₉: C, 47.83; H, 5.71; F, 8.73. Found: C, 48.68; H, 6.11; F, 6.89. GPC in CHCl₃ relative to polystyrene gave a monomodal distribution with M_n = 717 (M_w/M_n = 1.0).

Synthesis of Monomer 4b. Monosilanolisobutyl-POSS (**2b**) (1.5 g, 1.80 mmol) was used following the procedure outline for the preparation of **4a** to afford the title compound as a white solid (600 mg, 28%). Mp 61–63 °C; ATR-FTIR (neat) ν 2954 (m), 1591 (w), 1497 (w), 1280 (m), 1084 (vs), 791 (w) cm⁻¹; ¹H NMR (CDCl₃, 300 MHz) δ 7.64 (d, J = 8.9 Hz, 4H), 7.14 (d, J = 8.9 Hz, 4H), 1.94–1.78 (m, 7H), 1.16–0.95 (m, 42H), 0.79–0.60 (s, 17H); ¹³C NMR (CDCl₃, 75 MHz) δ 156.5, 135.9, 133.4, 115.2, 25.7, 23.9, 22.4, –0.9; ¹⁹F NMR (CDCl₃, 283 MHz) δ –119.5 (dd, J = 95.5, 55.4 Hz, *cis*-CF=CF₂, 2F), –126.4 (dd, J = 111.9, 95.5 Hz, *trans*-CF=CF₂, 2F), –133.8 (dd, J = 111.9, 52.4 Hz, CF=CF₂, 2F); ²⁹Si NMR (CDCl₃, 59 MHz) δ –9.6, –66.3, –67.3, –109.0 (1:3:4:1). Anal. Calcd for C₄₅H₇₄F₆O₁₅Si₉: C, 44.24; H, 6.10; F, 9.33. Found: C, 43.83; H, 6.33; F, 8.44. GPC in CHCl₃ relative to polystyrene gave a monomodal distribution with M_n = 948 (M_w/M_n = 1.0).

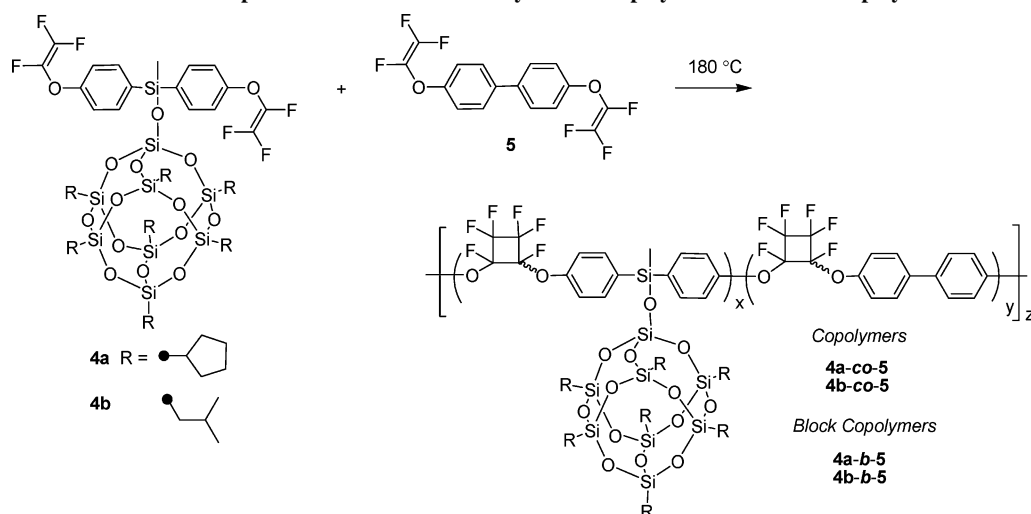
General Polymerization. In a vacuum-sealed glass ampule, a specified amount of **4a**, **4b**, and/or **5** were heated to 180 °C and for 48 h. After 48 h, the ampule was allowed to cool to room temperature, and the crude polymer was dissolved in a minimal amount of THF, then precipitated in methanol, filtered, washed repeatedly with methanol, and dried under vacuum to afford a pale yellow fibrous solid in nearly quantitative yield. For block copolymers **4b-b-5**, a weighed amount of prepolymer **poly4b** is heated with monomer **5** using the same procedure described above. Selected polymer properties (DSC, TGA, and GPC) data are reported in Table 1.

Analytical Data for Copolymer 4a-co-5. ATR-FTIR (neat) ν 2930 (w), 1495 (s), 1301 (s), 1194 (s), 1112 (s), 952 (vs), 821 (s) cm⁻¹; ¹H NMR (CDCl₃, 300 MHz) δ 7.48–7.40 (m, 8H), 7.26–

Scheme 2. Preparation of POSS TFVE Monomers (4a and 4b)



Scheme 3. Preparation of POSS PFCB Aryl Ether Copolymers and Block Copolymers



7.10 (m, 8H), 1.72–1.30 (m, 56H), 1.00–0.85 (m, 7H), 0.61 (s, 3H); ^{19}F NMR (CDCl_3 , 283 MHz) δ -126.5 to -136.7 (m, cyclobutyl- F_6).

Analytical Data for Copolymer 4b-co-5. ATR-FTIR (neat) ν 2930 (m), 1728 (vs), 1601 (w), 1490 (vs), 1288 (vs), 1200 (vs), 962 (vs), 825 (m), 742 (w) cm^{-1} ; ^1H NMR (CDCl_3 , 300 MHz) δ 7.52–7.40 (m, 8H), 7.26–7.10 (m, 8H), 1.86–1.81 (m, 7H), 0.95–0.89 (m, 42H), 0.60–0.53 (s, 17H); ^{19}F NMR (CDCl_3 , 283 MHz) δ -126.5 to -136.7 (m, cyclobutyl- F_6).

Analytical Data for Homopolymer poly4a. ATR-FTIR (neat) ν 2955 (m), 1593 (w), 1229 (m), 1115 (vs), 963 (m), 744 (m) cm^{-1} ; ^1H NMR (CDCl_3 , 300 MHz) δ 7.64 (m, 4H), 7.11 (m, 4H), 1.76–1.41 (m, 56H), 1.15–0.81 (m, 7H), 0.67 (s, 3H); ^{19}F NMR (CDCl_3 , 283 MHz) δ -119.4 (dd, J = 95.5, 55.4 Hz, *cis*- $\text{CF}=\text{CF}_2$, 2F), -126.2 (dd, J = 111.9, 95.5 Hz, *trans*- $\text{CF}=\text{CF}_2$, 2F), -126.5 to -136.7 (m, cyclobutyl- F_6), -133.8 (dd, J = 111.9, 52.4 Hz, $\text{CF}=\text{CF}_2$, 2F).

Analytical Data for Homopolymer poly4b. ATR-FTIR (neat) ν 2955 (m), 1595 (w), 1231 (m), 1118 (vs), 967 (m), 746 (m) cm^{-1} ; ^1H NMR (CDCl_3 , 300 MHz) δ 7.59–7.55 (m, 4H), 7.21–7.08 (m, 4H), 1.87–1.78 (m, 7H), 0.96–0.85 (m, 42H), 0.63–0.53 (s, 17H); ^{19}F NMR (CDCl_3 , 283 MHz) δ -119.3 (dd, J = 95.5, 55.4 Hz, *cis*- $\text{CF}=\text{CF}_2$, 2F), -125.9 (dd, J = 111.9, 95.5 Hz, *trans*- $\text{CF}=\text{CF}_2$, 2F), -127.7 to -131.2 (m, cyclobutyl- F_6), -131.7 (dd, J = 111.9, 52.4 Hz, $\text{CF}=\text{CF}_2$, 2F).

Analytical Data for Block Copolymer 4b-b-5. ATR-FTIR (neat) ν 2956 (w), 1606 (m), 1496 (s), 1304 (vs), 1199 (vs), 937

(vs), 760 (w) cm^{-1} ; ^1H NMR (CDCl_3 , 300 MHz) δ 7.59–7.55 (m), 7.21–7.08 (m), 1.87–1.76 (m, 7H), 0.99–0.84 (m, 42H), 0.61–0.55 (s, 17H); ^{19}F NMR (CDCl_3 , 283 MHz) δ -126.6 to -131.2 (m, cyclobutyl- F_6).

Results and Discussion

Monomer Synthesis. POSS-functionalized monomers **4a** (R = cyclopentyl) and **4b** (R = *iso*-butyl) were prepared by condensation of commercial monosilanolalkyl-POSS **2a** and **2b** with TFVE-functionalized chlorosilane (**3**) (Scheme 2). Silane (**3**) was prepared by a metal–halogen exchange with commercial 4-bromo(trifluorovinyl)benzene (**1a**).¹⁶ The aryl bromide of **1a** was initially transmetalated with an equivalent of *tert*-butyl lithium in a solution of diethyl ether at -79°C and produced quantitative conversion of the lithiated aryl trifluorovinyl ether intermediate (**1b**). (**Caution!** When warmed above -20°C , the aryl lithium intermediate **1b** primarily adds to the aryl trifluorovinyl ether and results in highly exothermic expulsion of LiF to re-form fluoroolefin species.)¹⁷ The lithiated intermediate was then reacted in situ with one-half equivalent of trichloromethylsilane affording **3**. Monomers **4a** and **4b** structures were elucidated by ^1H , ^{19}F , ^{13}C , and ^{29}Si NMR, and purity was confirmed by elemental combustion analysis (see Experimental Section). The melting point of the cyclopentyl POSS-functionalized monomer **4a** showed a significantly higher melting point

of 230 °C as compared to the *iso*-butyl POSS monomer **4b** with melting range of 61–63 °C. The trifluorovinyl ether moieties are typically thermally polymerized from 150 to 180 °C.⁴ The introduction of rigid cyclopentyl groups appended to the POSS cages of **4a** suppresses monomer melting; however, the monomer still undergoes thermal cyclodimerization in the bulk solid state forming PFCB aryl ether homopolymer **poly4a** after heating for 48 h at 180 °C.

Polymer Synthesis and Characterization. Copolymers (**4a-co-5** and **4b-co-5**) were prepared from the respective monomers by bulk polymerization at 180 °C producing POSS PFCB aryl ether copolymers (Scheme 3). The advantage of bulk polymerization is realized because monomer **5** has a reported melting point at 44–46 °C^{2b} and essentially serves as the solvent. In particular, monomer **5** easily dissolved the high melting (230 °C) cyclopentyl-functionalized POSS TFVE monomer **4a**. POSS PFCB aryl homopolymers were also prepared by thermal polymerization with monomers **4a** and **4b**, producing **poly4a** and **poly4b**, respectively, with an average of five POSS molecules in each chain segment ($n = 5$). POSS homopolymer **poly4b** was used to prepare block copolymer (**4b-b-5**) by thermal polymerization with monomer **5**. The preparation of a multiblock copolymer using **poly4a** and monomer **5**, by oligomerization of **4a** followed by copolymerization with monomer **5**, produced insoluble material that was difficult to characterize. DSC, TGA, and GPC analyses were performed on all polymers, and their selected properties are shown in Table 1.

GPC analysis revealed copolymers possessed similar number-average molecular weights with higher polydispersity indices (PDIs) as compared to the PFCB aryl ether homopolymer (**poly5**) at the same bulk, step-growth thermal polymerization conditions. In all copolymers prepared, the highest achievable POSS loading was 20 wt %; loadings higher than this produced phase separated, insoluble gels. Copolymer **4a-co-5** functionalized with 20 wt % POSS showed the highest polydispersity of 5.2. This may be likely due to the decreasing mobility of growing POSS PFCB aryl ether polymer chains causing a higher incidence of chain length fractionation. Because PFCB aryl ether thermal polymerizations are dependent on the rate of diffusion of aryl TFVEs, molecular weights are limited by melt viscosity. No POSS PFCB aryl ether macrocycles were observed via the intramolecular cyclodimerization of monomers (**4a** or **4b**) based on GPC analysis.

Polymer conversions were monitored using ¹⁹F NMR and GPC analysis (Figure 1). ¹⁹F NMR of copolymer **4b-co-5** with 20 wt % POSS exhibited the expected multiplet −130.0 to −135.5 ppm of the PFCB aryl ether ring from the thermal cyclodimerization with no evidence of residual aryl TFVE peaks of monomer **4a** or **5**. These are typically represented by an AMX pattern at −119.5 ppm (F_A), −126.4 ppm (F_M), and −133.8 ppm (F_X).

Thermal Properties. Differential scanning calorimetry (DSC) revealed a plasticizing effect demonstrated by lowered glass transition temperature (T_g) upon increased weight percent incorporation of POSS as expected and previously reported.¹⁵ The decrease was most notable for copolymers **4b-co-5** possessing POSS *iso*-butyl groups and further decreased with higher POSS loadings. As shown in Figure 2, there was a 14 °C decrease in T_g with POSS loading of 20 wt % in copolymer **4b-co-5** as compared to **poly5**. On the other hand, the rigid nature cyclopentyl-functionalized copolymer **4a-co-5** demonstrated a slight decrease in T_g with 20 wt % POSS loading. The block copolymers of **4b-b-5** showed an initial 8 °C increase in

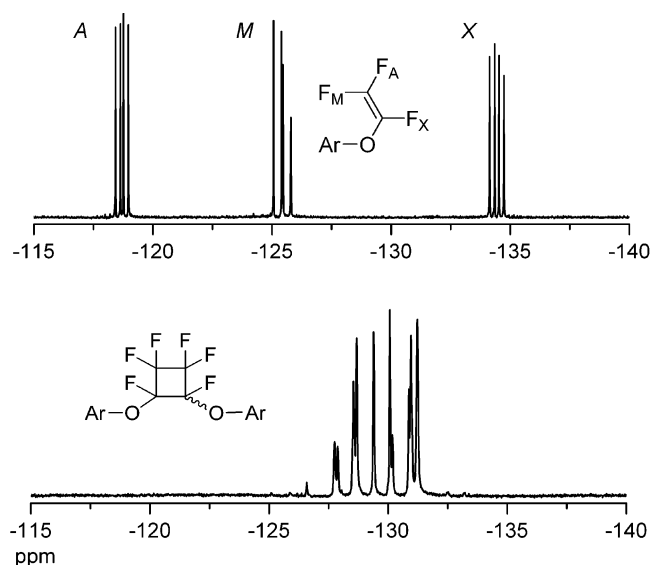


Figure 1. ¹⁹F NMR spectrum in CDCl₃ showing the conversion of POSS monomer **4b** (top) to 20 wt % POSS PFCB aryl ether copolymer **4b-co-5** (bottom).

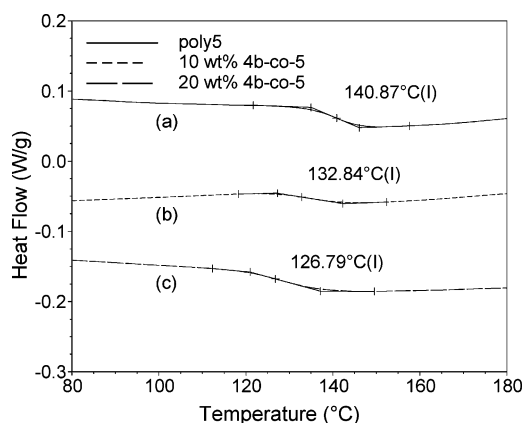


Figure 2. Third heating DSC scans in nitrogen (10 °C/min) overlay of (a) PFCB aryl ether homopolymer (**poly5**) as compared to (b) 10 wt % POSS PFCB aryl ether copolymer **4b-co-5** and (c) 20 wt % POSS PFCB aryl ether copolymer **4b-co-5**.

T_g for 10 wt % POSS, which then decreased upon 20 wt % POSS incorporation. The resulting drop in T_g from the incorporation of 20 wt % POSS may be due to the higher fraction of lower molecular weight chains observed by increased polydispersity. The thermal decomposition temperature (T_d) of the dried polymers was recorded using TGA in air and nitrogen. Their T_d was determined by initial mass loss at the onset temperature. Overall, high molecular weight POSS PFCB aryl ether copolymers **4a-c-5** and **4b-c-5** showed little deviation at onset in nitrogen and air as compared to PFCB aryl homopolymer **poly5**. The decomposition temperatures for homopolymers **poly4a-b** are not reported because they were only oligomerized to use as blocks in copolymerization and would not provide a reasonable comparison to the copolymers.

Polymer Film Surface Properties. Copolymers with up to 20 wt % *iso*-butyl-functionalized POSS produced optically transparent, creasable films. POSS loadings greater than 20 wt % produced polymers that were difficult to solution process. All polymers prepared can be solution processed either as spin cast films (SCF) or drop cast films (DCF) using common organics solvents such as THF or cyclopentanone.

The POSS PFCB aryl ether polymer films were studied using electron microscopy. Scanning electron microscopy (SEM) showed no evidence of micrometer-sized POSS aggregation.

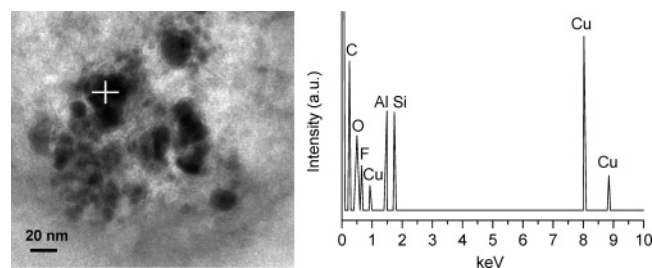


Figure 3. TEM micrograph on Cu/Al grid (left) of 20 wt % POSS PFCB aryl ether copolymer **4b-co-5** exposing nanometer-sized POSS aggregates, shown as dark areas. EDS (right) results of the TEM cross hair, confirming the enriched presence of silicon.

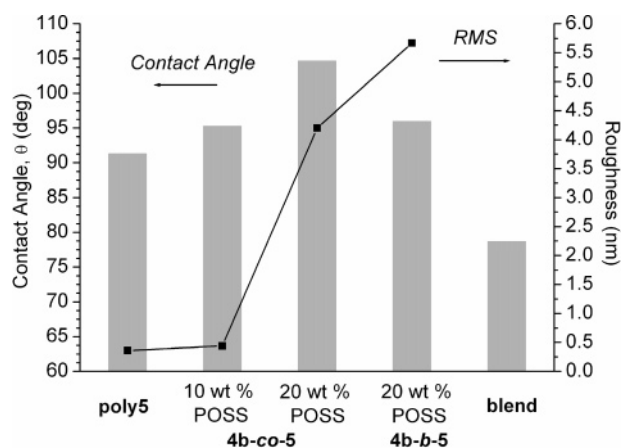


Figure 4. Water contact angle and surface roughness (rms) measurements of spin cast polymer films (SCF).

However, transmission electron microscopy (TEM) (Figure 3) revealed nanometer-sized POSS clusters with varying sizes ranging from 5 to 20 nm examined on various areas of the film surface, which were confirmed by energy dispersive X-ray spectroscopy (EDS) analysis. The observation also shows the discretely sized POSS cage aggregates are well dispersed within the bulk PFCB aryl ether polymer.

The hydrophobicity of the copolymer films of **4b-co-5** was tested using water drop shape analysis and measured for the corresponding contact angle (θ) (Figure 4). The relationship of contact angle and surface energy is governed by Young's equation that relates interfacial tensions between the surface of the liquid and gas phase of water.¹⁸ Furthermore, it is well known that surface roughness imparts increased hydrophobicity as demonstrated by Cassie and Wenzel.¹⁹

As compared to the homopolymer **poly5**, copolymer **4b-co-5** showed modest increases in water contact angle with increasing POSS content. The highest increase in water repellency was 16% for 20 wt % POSS copolymer **4b-co-5** with an average contact angle of $104.7^\circ (\pm 0.6^\circ)$ as compared to homopolymer **poly5** that averaged $91.3^\circ (\pm 1.2^\circ)$. Furthermore, block copolymer **4b-b-5** showed no deviation in water contact angle within error as compared to that of **poly5**. Using 3D white light optical profilometry, the degree of surface roughness showed good correlation with increasing water contact angles. As shown in Figure 5, images obtained from optical profilometry revealed significant surface roughening of the 20 wt % POSS PFCB aryl ether copolymer **4b-co-5** as compared to homopolymer **poly5** with an average surface roughness (rms) of 4.2 and 0.4 nm, respectively. The incorporation of POSS increased the surface roughness up to 12–19 times as compared to that of the homopolymer films. The average sizes of the surface protrusions were measured as the peak-to-valley ratio and were 38.0 nm

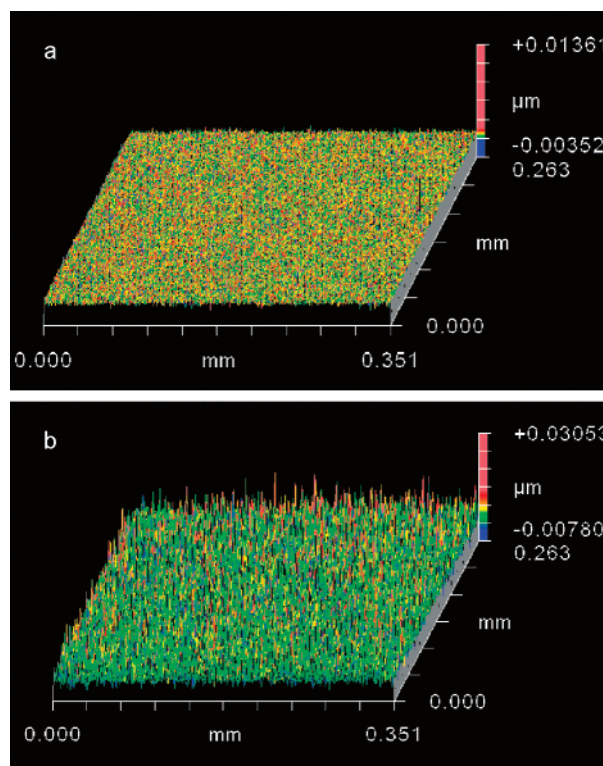


Figure 5. 3D surface projections of **poly5** (a) and copolymer **4b-co-5** (b) obtained from white light optical profilometry.

for **4b-co-5** and 17.0 nm for **poly5**. As a further comparison, 20 wt % of fully condensed octaisobutyl-POSS (*i*-Bu₈T₈ POSS) was solvent blended (THF) with **poly5** and spin cast as a film (denoted **blend** in Figure 4). The resulting film's water contact angle was 15% lower as compared to PFCB aryl homopolymer **poly5** and produced a white opaque, phase separated film. Therefore, as compared to the POSS PFCB aryl ether copolymers, it is evident the covalently bound POSS demonstrated better compatibility over the POSS blended material.

It was recently shown that POSS covalently bound into polyurethanes improves dewetting, due to the increase in the nanometer surface roughness as well as hydrophobic alkyl groups on the POSS structures.²⁰ Furthermore, the existence of nanometer surface roughness has been shown to theoretically and experimentally contribute analogous hydrophobic behavior similar to that caused by the micrometer relief texture of the lotus leaf, albeit with less magnitude.²¹

Our results are consistent with this observation in that the surface roughening due to the presence of hydrophobic, nanometer-sized POSS molecules attributes a modest increase in hydrophobicity. The hydrophobicity can be further influenced by the substitution of the alkyl substituents on the POSS cages with fluorinated alkyl chains, which has been demonstrated with 3,3,3-trifluoropropyl-functionalized POSS encapped poly(methylmethacrylates).²²

Conclusions

We have synthesized and characterized PFCB aryl ether copolymers and multiblock copolymers with pendant cyclobutyl- and *iso*-butyl-functionalized POSS cages. The facile preparation of the corresponding POSS TFVE monomers **4a** and **4b** was achieved utilizing the aryl TFVE lithium intermediate **1b** followed by successive condensation with commercial monosilanolalkyl POSS. These POSS PFCB aryl ether copolymers demonstrated excellent solution processability producing opti-

cally transparent, flexible films. DSC analysis of T_g 's revealed a plasticizing effect upon incorporation of iso-butyl POSS as random PFCB aryl ether copolymers and block copolymers, whereas the cyclopentyl POSS PFCB aryl ether copolymers showed negligible changes. Incorporation of POSS showed no change in thermal stability as compared to the PFCB aryl ether homopolymer as demonstrated by TGA analysis. Furthermore, POSS incorporation into the PFCB aryl ether fluoropolymer produced unique surface features when cast as films showing increased surface roughness that ultimately improved hydrophobicity. We anticipate the functionalization of PFCB aryl ether polymers with fluorinated POSS cages would further improve the water repellency. We find the ability to solution process these POSS-functionalized fluoropolymers makes them particularly attractive for a broad range of manufacturing techniques for potential hydrophobic material applications including fibers, coatings, and bulk components.

Acknowledgment. We thank the National Science Foundation (DMR 0514622), Defense Advanced Research Projects Agency (DARPA), and the Department of Energy (BES DE-FG02-05ER15718) for financial support. J.M.M. also acknowledges partial support from the Air Force Office of Scientific Research (AFOSR). S.T.I. gratefully acknowledges the United States Air Force Institute of Technology Civilian Institutions program for sponsorship. We thank S. Gaylord and Dr. K. Richardson (CU) for optical profilometry measurements. Dr. J. Hudson is acknowledged for microscopy support through the Electron Microscope (EM) facility at CU. We also thank Dr. Timothy Haddad (AFRL) and Dr. Chris Topping (Tetramer Technologies) for technical assistance.

References and Notes

- (1) *Modern Fluoropolymers: High Performance Polymers for Diverse Applications*; Scheirs, J., Ed.; Wiley: Chichester, 1997.
- (2) (a) For a recent review, see: Iacono, S. T.; Budy, S. M.; Jin, J.; Smith, D. W., Jr. *J. Polym. Sci., Part A: Polym. Chem.* **2007**, *45*, 5707. (b) Babb, D. A.; Ezzell, B. R.; Clement, K. S.; Richey, W. F.; Kennedy, A. P. *J. Polym. Sci., Part A: Polym. Chem.* **1993**, *31*, 3465.
- (3) Smith, D. W., Jr.; Chen, S.; Kumar, S.; Ballato, J.; Shah, H.; Topping, C.; Foulger, S. H. *Adv. Mater.* **2002**, *14*, 1585.
- (4) (a) Cheatham, C. M.; Lee, S.-N.; Laane, J.; Babb, D. A.; Smith, D. W., Jr. *Polym. Int.* **1998**, *46*, 320. (b) Spraul, B. K.; Suresh, S.; Jin, J.; Smith, D. W., Jr. *J. Am. Chem. Soc.* **2006**, *128*, 7055. (c) The diradical intermediate has recently been observed by EPR. See: Misfud, N.; Mellon, V.; Jin, J.; Topping, C. M.; Echegoyen, L.; Smith, D. W., Jr. *Polym. Int.* **2007**, *56*, 1142.
- (5) (a) Spraul, B. K.; Suresh, S.; Glaser, S.; Perahia, D.; Ballato, J.; Smith, D. W., Jr. *J. Am. Chem. Soc.* **2004**, *126*, 12772. (b) Jiang, X.; Liu, S.; Liu, M. S.; Herguth, P.; Jen, A. K.-Y.; Fong, H.; Sarikaya, M. *Adv. Funct. Mater.* **2002**, *12*, 745. (c) Ghim, J.; Lee, D.-S.; Shin, B. G.; Vak, D.; Yi, D. K.; Kim, M.-J.; Shim, H.-S.; Kim, J. J.; Kim, D.-Y. *Macromolecules* **2004**, *37*, 5724.
- (6) (a) Luo, J.; Liu, S.; Haller, M.; Liu, L.; Ma, H.; Jen, A. K.-Y. *Adv. Mater.* **2002**, *13*, 1763. (b) Ma, H.; Sen, L.; Luo, J.; Suresh, S.; Liu, L.; Kang, S. H.; Haller, M.; Sassa, T.; Dalton, L. R.; Jen, A. K.-Y. *Adv. Funct. Mater.* **2002**, *12*, 565.
- (7) Jin, J.; Smith, D. W., Jr.; Topping, C.; Suresh, S.; Chen, S.; Foulger, S. H.; Rice, N.; Mojazza, B. *Macromolecules* **2003**, *36*, 9000.
- (8) (a) Perpall, M. W.; Smith, D. W., Jr.; DesMarteau, D. D.; Creager, S. E. *J. Macromol. Sci., Part C: Polym. Rev.* **2006**, *46*, 297. (b) Ford, L. A.; DesMarteau, D. D.; Smith, D. W., Jr. *J. Fluorine Chem.* **2005**, *126*, 653.
- (9) Gonzales, R. I.; Phillips, S. H.; Hoflund, G. B. *J. Spacecraft Rockets* **2000**, *37*, 463.
- (10) Phillips, S. H.; Haddad, T. S.; Tomczak, S. J. *Curr. Opin. Solid State Mater. Sci.* **2004**, *8*, 21.
- (11) (a) Laine, R. M. *J. Mater. Chem.* **2005**, *15*, 3725. (b) Li, G.; Wang, L.; Ni, H.; Pittman, C. U., Jr. *J. Inorg. Organomet. Polym.* **2001**, *11*, 123. (c) Provatas, J. G.; Matisons, J. G. *Trends Polym. Sci.* **1997**, *5*, 327. (d) Baney, R. H.; Itoh, M.; Sakakibara, A.; Suzuki, T. *Chem. Rev.* **1995**, *95*, 1409. (e) Loy, D. A.; Shea, K. J. *Chem. Rev.* **1995**, *95*, 1431. (f) Voronkov, M. G.; Lavrent'yev, V. I. *Top. Curr. Chem.* **1982**, *102*, 199.
- (12) Suresh, S.; Zhou, W.; Spraul, B.; Laine, R. M.; Ballato, J.; Smith, D. W., Jr. *J. Nanosci. Nanotechnol.* **2004**, *4*, 250.
- (13) (a) Smith, D. W., Jr.; Babb, D. A. *Macromolecules* **1996**, *29*, 852. (b) Rizzo, J.; Harris, F. W. *Polymer* **2000**, *41*, 5125.
- (14) Ghim, J.; Baeg, K.-J.; Noh, Y.-Y.; Kang, S.-J.; Jo, J.; Kim, D.-Y.; Cho, S.; Yuen, J.; Lee, K.; Heeger, A. J. *Appl. Phys. Lett.* **2006**, *89*, 202516.
- (15) Iacono, S. T.; Budy, S. M.; Mabry, J. M.; Smith, D. W., Jr. *Polymer* **2007**, *48*, 4637.
- (16) Ji, J.; Narayan-Sarathy, S.; Neilson, R. H.; Oxley, J. D.; Babb, D. A.; Tondan, N. G.; Smith, D. W., Jr. *Organometallics* **1998**, *17*, 783.
- (17) Nucleophilic addition–elimination transformations of fluoroolefins are a well-established area of organofluorine chemistry. For a comprehensive review of this literature, see: Chambers, R. D. In *Synthetic Fluorine Chemistry*; Olah, G. A.; Surya Prakash, G. K., Eds.; Wiley & Sons: New York, 1992; p 359. See also ref 16.
- (18) Young, T. *Philos. Trans. R. Soc.* **1805**, *95*, 65.
- (19) (a) Cassie, A. B. D.; Baxter, S. *Trans. Faraday Soc.* **1944**, *40*, 546. (b) Wenzel, R. N. *Ind. Eng. Chem.* **1936**, *28*, 988.
- (20) Turri, S.; Levi, M. *Macromol. Rapid Commun.* **2005**, *26*, 1233.
- (21) (a) Zhu, L.; Xiu, Y.; Xu, J.; Tamirisa, P. A.; Hess, D. W.; Wong, C.-P. *Langmuir* **2005**, *21*, 11208. (b) Pal, S.; Weiss, H.; Keller, H.; Müller-Plather, F. *Langmuir* **2005**, *21*, 3699. (c) Rios, P. F.; Dodiuk, H.; Kenig, S.; McCarthy, S.; Dotan, A. *J. Adhes. Sci. Technol.* **2006**, *20*, 563.
- (22) Koh, K.; Sugiyama, S.; Morinaga, T.; Ohno, K.; Tsujii, Y.; Fukuda, T.; Yamahiro, M.; Iijima, T.; Oikawa, H.; Wantanabe, K.; Miyashita, T. *Macromolecules* **2005**, *38*, 1264.

MA071732F